horticulturae

MDPI

Article

Foliar Application of Protein Hydrolysates Promotes Growth and Affects Leaf Ionome in Olive

Igor Pasković [1], Maša Andlovic [2], Helena Plešnik [3], Primož Vavpetič [3], Paula Žurga [4], Ljiljana Popović [5], Martin Šala [6], Mario Franić [1], Ivan Dlačić [1], Smiljana Goreta Ban [1], Marija Polić Pasković [1,*], Tina Kosjek [3] and Paula Pongrac [2,3]

[1] Institute of Agriculture and Tourism, Karla Huguesa 8, 52440 Poreč, Croatia; paskovic@iptpo.hr (I.P.); mario@iptpo.hr (M.F.); ivan@iptpo.hr (I.D.); smilja@iptpo.hr (S.G.B.)
[2] Biotechnical Faculty, University of Ljubljana, Jamnikarjeva 101, 1000 Ljubljana, Slovenia; masa.andlovic@bf.uni-lj.si (M.A.); paula.pongrac@bf.uni-lj.si (P.P.)
[3] Jožef Stefan Institute, Jamova cesta 39, 1000 Ljubljana, Slovenia; helena.plesnik@ijs.si (H.P.); primoz.vavpetic@ijs.si (P.V.); tina.kosjek@ijs.si (T.K.)
[4] Teaching Institute of Public Health of Primorsko-Goranska County, Krešimirova 52a, 51000 Rijeka, Croatia; paula.zurga@zzjzpgz.hr
[5] Faculty of Technology, University of Novi Sad, Bulevar cara Lazara 1, 21000 Novi Sad, Serbia; ljiljana04@tf.uns.ac.rs
[6] National Institute of Chemistry, Hajdrihova 18, 1000 Ljubljana, Slovenia; martin.sala@ki.si
* Correspondence: mpolic@iptpo.hr

Abstract

The foliar application of various biostimulants, such as protein hydrolysates (PHs), has been associated with improved nutrient uptake efficiency and stress tolerance in perennial crops, like olive (*Olea europaea* L.). In this study, PHs obtained by enzymatic hydrolysis by Alcalase Pure (referred to as treatment H1), Alcalase Pure and Flavourzyme (referred to as treatment H2), or Alcalase Pure and Protana™ Prime (referred to as treatment H3) with proteins from pumpkin seed cake were tested for their potential beneficial growth, performance, and nutrition effects in one-year-old olive seedlings grown under controlled conditions. Amino acid and element compositions were evaluated in the PHs, which were used for foliar application six times at eight-day intervals. Control (C) plants were treated the same way, but without PHs. Shoot and root growth, leaf reflectance indices, and the composition of micro and macronutrients in different organs and leaf tissues were determined. Plants in the H2 treatment grew significantly better than C plants. They had the highest Photochemical Reflectance Index and a Chlorophyll-Normalized Difference Vegetation Index similar to that of C plants, indicating an optimal growth/photosynthesis balance. A decrease in the concentration of several mineral elements in the lower epidermis in H2- and H3-treated plants compared to C and H1-treated plants was accompanied by their increase in the spongy mesophyll, indicating their redistribution to support increased metabolism, resulting in increased shoot growth in these two treatments. Arguably, these observed effects could be attributed to the amino acid profile of the H2 mixture, which had the highest concentration of L-proline, L-arginine, and L-lysine among the three PH mixtures, and a higher L-asparagine concentration than the H1 mixture. Overall, the results highlight the applicative potential of tailored PH formulations for the optimization of growth, mineral element composition, and physiological performance in olive cultivation.

Keywords: hydrolyzed proteins; pumpkin cake; biostimulants; element localization; olive cultivation

Academic Editor: Yang Liu

Received: 3 December 2025
Revised: 22 January 2026
Accepted: 27 January 2026
Published: 29 January 2026

1. Introduction

Cultivation of olives (*Olea europaea* L.) is the basis of Mediterranean agriculture and is tightly linked with the local economy and cultural heritage. In addition to olive fruits and olive oil, various by-products of olive cultivation, such as twigs, leaves, and pomace, all rich in bioactive compounds, have been integrated into the production of functional foods, food supplements, phytochemicals, and nutraceuticals [1]. The long-term sustainability of olive production is being perturbed by unpredictable climate changes, which are exacerbating soil degradation, depleting water resources, and facilitating the emergence of new pathogens [2,3]. Among the factors enabling stable olive cultivation under these stress conditions is the nutritional status of olive trees, as this ensures optimal vegetative and reproductive growth while enhancing resilience. Therefore, research exploring the links between olive leaf nutrition and stress has attracted significant interest [4].

In this context, biostimulants, i.e., substances or microorganisms that stimulate natural processes to enhance nutrient uptake, nutrient-use efficiency, stress tolerance, and crop quality, regardless of their nutrient content [5], have been extensively explored as innovative tools for enhancing plant growth and improving stress tolerance. Du Jardin [6] highlighted that biostimulants seem to offer a unique opportunity to bridge plant nutrition and plant health, emphasizing the need to extend 'plant care' to the strengthening of the plants' capacity to withstand adverse environments and to cope with the scarcity of nutrients and water resources, which are all challenges amplified by climate change. Among the seven main categories of biostimulants, protein hydrolysates (PHs) have been shown to enhance crop performance, particularly under stressful environmental conditions [7,8]. This ability has been attributed to a higher ratio of peptides to free amino acids and a greater proportion of L-amino acids obtained from the enzymatic hydrolysis of plant-derived PH mixtures compared to animal-derived PHs, which are typically produced by acid hydrolysis [8].

General modes of indirect action in biostimulants remain poorly resolved because of the complexity of factors such as the quality and composition of proteins from different plant sources, the enzymes used, the conditions of hydrolysis, the methods of application, and the types of stress. Combining mineral fertilizers, biofertilizers, or different biostimulants (including amino acids) in olive orchards has already been shown to improve fruit and olive oil quality [9] simultaneously. This is presumably a consequence of (in)directly optimizing the supply of essential mineral nutrients and/or other regulators of plant metabolism supporting the physiological and biochemical processes that drive growth, flowering, fruit set, and oil accumulation [10]. In a conventional olive orchard, the most applied nutrient is nitrogen (N), which, due to its role in protein and chlorophyll synthesis, promotes photosynthesis and yield [11]. By contrast, phosphorus (P) deficiency is not very common in olive orchards, while potassium (K) deficiency is considered the most prevalent nutritional disorder in rainfed olive cultivation [10]. Through the key involvement of K in stomatal regulation, osmotic adjustment, and carbohydrate distribution, K nutritional status in olives critically contributes to drought stress resilience [12,13], and, through interactions with amino acid metabolism and the stimulation of IAA-oxidase activity, K affects flowering [11]. Calcium (Ca) is essential for maintaining plant structural integrity and preventing pathogen entry, while magnesium (Mg), as part of chlorophyll, plays a crucial role in photosynthesis [14], but they are rarely applied. Sulphur (S) is an essential nutrient for many physiological functions, such as protein synthesis and enzyme activation [15]. It therefore affects the biosynthesis of different primary and secondary metabolites, which are vital for plant growth and development [14]. Micronutrients such as iron (Fe), manganese (Mn), copper (Cu), and zinc (Zn) are essential for enzymatic activity and metabolic regulation [14,16], with boron (B) supporting olive reproductive development [17], and these are also seldom used to improve olive production. Deficiencies or imbalances in any of

these nutrients impair tree vigor, fruiting, and oil quality, and can increase susceptibility to diseases such as olive leaf spot [4].

This study investigated the effects of the foliar application of PHs obtained by the enzymatic hydrolysis of pumpkin (*Cucurbita pepo* var. styriaca) seed cake proteins and assessed their impact on the shoot and root growth of one-year olive seedlings, leaf reflectance, and the composition of micro and macronutrients in different organs and leaf tissues. We hypothesize that tailored PHs will enhance growth and modulate ionome distribution in olive seedlings.

2. Materials and Methods

2.1. Protein Hydrolysates and Their Characterization

Proteins were isolated from pumpkin seed cake, as previously described in detail [18]. This protein isolate was hydrolyzed with the enzymes Alcalase® Pure (Novozymes, Bagsværd, Denmark, treatment referred to as H1), enzymes Alcalase® Pure and Flavourzyme® (Novozymes, Bagsværd, Denmark, treatment referred to as H2), or enzymes Alcalase® Pure and Protana™ Prime® (Novozymes, Bagsværd, Denmark, treatment referred to as H3). First, a suspension of 1.5 g of isolated proteins in 100 mL was prepared by suspending the required amount of protein isolates in 0.2 mol L^{-1} TRIS–HCl buffer solution at pH 9.0. Enzymatic hydrolysis was carried out at 50 °C for 180 min with an enzyme-to-substrate ratio of 1/50. The degree of hydrolysis was determined by the trichloroacetic acid method: the obtained suspension of hydrolyzed proteins was mixed with trichloroacetic acid (0.44 mol L^{-1}) in a 1:1 volume ratio and incubated at 4 °C for 30 min, after which the mixture was centrifuged (Eppendorf miniSpin Plus (Eppendorf, Hamburg, Germany), 14,500 rpm, 10 min). Protein content was determined in both fractions using the method described by [18], with bovine serum albumin as the standard protein. The degree of hydrolysis was calculated as the ratio of 0.22 mol L^{-1} trichloroacetic acid-soluble proteins to total proteins in the hydrolysate, expressed as a percentage.

Characterization of the PHs used in this study comprised targeted and non-targeted amino acid and dipeptide profiling and element composition assessment. For targeted and non-targeted amino acid and dipeptide analysis, ammonium formate and formic acid were purchased from Sigma Aldrich (St Louis, MO, USA), LC-MS-grade acetonitrile (ACN) and LC-MS-grade water were purchased from J. T. Baker (Phillipsburg, NJ, USA) and the amino acid standards (≥98%) used for analysis included L-valine, L-leucine, L-isoleucine, L-threonine, L-serine, L-proline, L-methionine, L-glutamic acid, L-phenylalanine, L-lysine, L-tyrosine, 4-Aminobutyric acid, L-asparagine, L-glutamine, L-cysteic acid, glycine, and L-arginine (all Sigma Aldrich). The internal standard, Stable Isotope Labeled Amino Acid Mix Solution 1, containing labeled variants of 17 amino acids, was obtained from Supelco (Buchs, Switzerland). The samples were prepared by 10-time dilution with acetonitrile containing 10% Milli-Q water. A mixture of isotopically labeled amino acids was added as an internal standard to each sample, yielding a final concentration of 500 µg L^{-1}. Calibration standards were prepared at concentrations of 10, 50, 100, 250, 500, and 750 µg L^{-1} of each amino acid. The internal standard mixture was added to all calibration levels in the same way as for the samples.

Chromatographic separation was performed on a Vanquish UHPLC system (Thermo Fisher Scientific, Waltham, MA, USA) using an Acquity BEH Amide column (Waters, 2.1 × 100 mm, 1.7 µm) maintained at 35 °C. Mobile phase A consisted of acetonitrile, and mobile phase B of 20 mM ammonium formate with 0.1% formic acid. The gradient program was as follows: 0–2 min, 10% B; 2–16 min, 10–45% B; 16–17 min, 45–10% B; followed by re-equilibration at 10% B until 30 min. The flow rate was 0.40 mL $min^{-1,}$ and the injection volume was 5 µL. Mass spectrometric detection was performed using a high-resolution

Orbitrap instrument (Thermo Fisher Scientific, Waltham, MA, USA) equipped with a heated electrospray ionization (HESI) source. The instrument was operated in either positive or negative ionization mode, using identical acquisition settings, except for polarity. The spray voltage was 3500 V, and the sheath, auxiliary, and sweep gas flows were 50, 50, and 1 (arbitrary units), respectively. The ion transfer tube and vaporizer temperatures were 325 °C and 350 °C. EASY-IC™ internal calibration and Advanced Peak Determination were enabled. Full MS scans were acquired at 120,000 resolving power (m/z 200) over m/z 70–1000 in centroid mode. Data-dependent MS/MS (dd-MS^2) was performed with eight dependent scans per cycle, using a 1.5 m/z isolation window and stepped HCD energies of 30, 50, and 150, recorded at 30,000 resolving power. Dynamic exclusion was enabled (repeat count 1, exclusion duration 9 s, ±5 ppm tolerance, isotopes excluded).

Data processing was performed in MZmine 4.8.0 using the following workflow: (i) mass detection with noise levels set to 50,000 for MS^1 and 25,000 for MS^2; (ii) chromatogram building with a minimum of 5 consecutive scans, a minimum consecutive-scan intensity of 50,000, a minimum absolute peak height of 50,000, and an m/z tolerance of 0.0020 m/z or 10.0 ppm; (iii) retention-time smoothing using the Savitzky–Golay algorithm; (iv) peak deconvolution using the Local Minimum feature resolver with an 85% chromatographic threshold, a minimum RT search range of 0.15 min, a minimum absolute height of 50,000, a minimum peak-top-to-edge ratio of 2.0, a peak duration range of 0.00–4.51 min, and a minimum of 4 scans per feature; (v) ^{13}C isotope filtering with an m/z tolerance of 3.0 ppm, an RT tolerance of 0.20 min, a maximum charge state of 1, and assignment of the most intense isotope as the representative feature; (vi) join aligner with an m/z tolerance of 0.0015 m/z or 5.0 ppm, an RT tolerance of 0.5 min, with no requirement for matching charge state or identification and without isotope-pattern or spectral-similarity comparison; (vii) peak finder with 1% intensity tolerance, m/z tolerance of 0.0010 m/z or 5.0 ppm, RT tolerance of 0.5 min, and a minimum of 4 scans; and (viii) duplicate peak filtering using the "new average" mode with an m/z tolerance of 0.0008 m/z or 1.5 ppm and an RT tolerance of 0.10 min. Feature heights were first normalized using the closest eluting IS (normalized intensities).

For targeted analysis, quantitative measurements of amino acids for which authentic standards were available were performed, and calibration curves were prepared. Identification was confirmed by matching retention time and MS/MS spectra to the injected standards (Schymanski level 1) [19]. Calibration curves were fitted using linear regression; valine showed an R^2 of 0.94, whereas all other amino acids exhibited R^2 values of 0.99 or higher. The LLOQ was defined as the lowest calibration level with S/N > 3.

For non-targeted analysis, MS/MS spectra were matched against the MoNA (MassBank of North America) experimental library using the same mass-accuracy criteria as in the targeted workflow (precursor < 5 ppm; fragments < 10 ppm). These features were reported at Schymanski's level 2 confidence [19]. Annotation was restricted to di- and tripeptides, and matches outside this compound class were not reported.

Concentrations of Mg, K, Ca, Mn, Fe, Cu, Zn, and B in PHs were determined directly in PHs using inductively coupled plasma mass spectrometry, as described previously [20].

2.2. Experimental Setup and Plant Material

Sixteen one-year-old olive (*Olea europaea* L. cv. Leccino) seedlings, purchased from Darko Nursery (Rovinj, Croatia) as certificated plant material, were potted into 3.5 L pots filled with perlite and Potground H (Klasmann-Deilmann GmbH, Geeste, Germany) substrate mixture (1/3 v/v). Their leaves were carefully washed with a paper towel moistened with distilled water to remove visible deposits. Plants were allowed to acclimatize to a 12/12 day/night cycle with a 25/15 °C temperature regime for two weeks before start-

ing the foliar treatments, which were applied six times at eight-day intervals. Each time, the plants were entirely sprayed with approximately 200 mL of the solution until runoff. Control plants (C) received a treatment consisting of distilled water with a wetting agent (0.15 mL L^{-1}; Optimus, AgroChem Max, Zagreb, Croatia), whereas PH-treated plants received distilled water, the same wetting agent, and the H1, H2, or H3 hydrolysates, diluted so that each solution contained 1.2 g L^{-1} of total soluble proteins. After spraying, all four plants per treatment were allowed to dry, then arranged in a randomized complete block design. At the start and at the end of the experiment, the elongation of the central shoot was measured. Eight days after the final foliar application, the six leaf reflectance indices listed in Table 1 were measured using the CI-710 SpectraVue Leaf Spectrometer (CID Bio-Science Inc., Camas, WA, USA), and plants were harvested. One leaf per plant (yielding four leaves per treatment) was sampled for tissue-specific elemental analysis and prepared by cryo-fixation, cryo-sectioning, and freeze-drying, as described previously [21]. To minimize the within-leaf variation, pieces of leaves (circa 5 × 5 mm^2) were sampled on the same leaf area, namely on the bottom half of the leaf, including the main vein and the neighboring leaf blade. For bulk analyses, shoots were separated into young leaves (i.e., those that developed during the experiment), old leaves, and stems; washed with tap water, then with distilled water containing 1% acetic acid, and finally with distilled water; frozen in liquid nitrogen; and freeze-dried at −96 °C and 0.0012 mbar for three days in Scanvac, CoolSafe (LaboGene, Allerød, Denmark). Roots were gently removed from the substrate, carefully washed, and scanned using WinRhizo software (version 2017a, Quebec City, QC, Canada) for morphological analysis: root length, root surface area, root volume, and average root diameter were measured, and then the roots were oven-dried at 35 °C for three days until reaching a constant mass [22].

Table 1. Overview of reflectance indices and calculation formulas, with data ranges, according to the internal firmware index definitions of the CI-710 SpectraVue Leaf Spectrometer (CID Bio-Science, Camas, WA, USA).

Index	Full Name	Formula	Range During Vegetation
CNDVI	Chlorophyll-Normalized Difference Vegetation Index	$(W_{750} - W_{705})/(W_{750} + W_{705})$	−1 to 1 (commonly 0.2–0.8)
PRI	Photochemical Reflectance Index	$(W_{531} - W_{570})/(W_{531} + W_{570})$	−1 to 1 (commonly −0.2–0.2)
GI	Greenness Index	W_{554}/W_{677}	–
SIPI	Structure Insensitive Pigment Index	$(W_{800} - W_{445})/(W_{800} + W_{680})$	0–2 (commonly 0.8–1.8)
WBI	Water Band Index	W_{900}/W_{970}	0.8–1.2
PSRI	Plant Senescence Reflectance Index	$(W_{680} - W_{500})/W_{750}$	−1 to 1 (commonly −0.1–0.2)

2.3. Bulk Element Analysis in Plant Material

All plant material was ground and homogenized to a fine powder using a 0.2 mm sieve in the Ultra Centrifugal mill ZM 200 (Retsch Maschinen GmbH, Setzingen, Germany). As described previously [1], a precisely measured 0.200 g of plant material was digested with 5 mL of 65% HNO_3 at 200 °C for 20 min using a Multiwave 3000 (Anton Paar, Graz, Austria), then diluted to 25 mL with ultrapure water. Manganese, Cu, Fe, Zn, and B were determined by inductively coupled plasma mass spectrometry (NexION 300X, PerkinElmer, Shelton, CT, USA), and Ca, K, and Mg by flame atomic absorption spectrometry (AAS800, PerkinElmer). Calibration utilized certified standards; only curves with an R^2 value greater than 0.999 were accepted.

2.4. Leaf Tissue-Specific Element Analysis

Quantitative distribution of P, S, chlorine (Cl), K, Ca, Mn, Fe, Cu, and Zn in cross-sections of leaves was determined using micro-proton induced X-ray emission (micro-PIXE) at the ion accelerator (High Voltage Engineering Europa B.V., Amersfoort, The Netherlands) of the Jožef Stefan Institute (Ljubljana, Slovenia) as described previously [21]. In short, accelerated protons were focused to approximately 1×1 μm^2 beam size, scanning the sections sandwiched between the Pioloform foils stretched over an aluminum holder placed in a vacuum chamber. The interaction between protons and atoms in the sample induces X-ray emissions characteristic of each element. X-rays were detected by a four-segmented SDD detector (PNDetector, Münich, Germany), and spectra were recorded using Oxford Microbeam Data Acquisitio-3 (OMDAQ-3, Oxford Microbeams Ltd., Bicester, UK) software, which saves pixel-by-pixel spectra in a list mode file. These spectra were processed in GeoPIXE II software [23], where distribution maps were generated, and ASCII files with pixel-by-pixel concentrations in a matrix were exported. Tissue-specific concentrations were extracted from these matrices using Fiji (version 1.54p) [24] by importing as a Text Image followed by selecting the cell type (i.e., tissue) in the image—namely the whole section (W), upper epidermis (UE), lower epidermis (LE), palisade mesophyll (PM), and spongy mesophyll (SM—as previously described in detail [21]); using the Brush tool; and saving the selection to the Region of Interest Manager to calculate average concentrations in the selected tissues. Epidermises were selected based on Ca maps, considering the outermost layer of the sample, while mesophylls were discerned based on S distribution maps, namely, palisade mesophyll was recognized by its high S concentration and elongated structures (cells), while spongy mesophyll comprised the remaining area of the leaf, with lower S concentrations and more round structures (cells). None of the tissues were overlapping in this selection.

2.5. Statistical Analysis

Bar charts displaying means (n = 4) ± standard errors were generated using SigmaPlot version 12.0 (Systat Software, San Jose, CA, USA). Statistical analyses were performed using TIBCO Statistica version 14.1.0.8 (TIBCO StatSoft, Palo Alto, CA, USA). Data were analyzed using a randomized complete block design (RCBD), with treatment as the main effect and replicates included as blocks. The use of four biological replicates per treatment (n = 4), with each replicate corresponding to a single plant, follows a previously used experimental approach in olive studies, in which individual plants were treated as independent experimental units [1,21]. In the present study, replication and total number of seedlings were additionally constrained by the physical capacity of the growth chamber and the strong focus on micro-PIXE analysis, which requires extensive beam time per sample and therefore inherently limits the number of analyzable specimens. Normality was assessed on ANOVA residuals using Q–Q plots and the Shapiro–Wilk test, whereas homogeneity of variances was evaluated using Levene's type-test based on absolute ANOVA residuals [25]. When ANOVA assumptions were satisfied for the original or transformed data, parametric RCBD ANOVA followed by Fisher's least significant difference (LSD) test was applied ($p < 0.05$). If assumptions were still violated after transformation, the original data were rank-transformed and analyzed using RCBD ANOVA on ranks, as commonly applied in ecological studies [26], with Bonferroni-adjusted pairwise comparisons. Post hoc power analyses for leaf tissue and plant organ-specific elemental concentrations were performed in R (version 4.4.1) [27] using RStudio (version 2024.09.0) [28] and are reported in Supplementary Table S1.

3. Results

First, we characterized the amino acid, peptide, and mineral element compositions of the PHs used in the experiment. The amino acid compositions of the three PH treatments revealed apparent differences between these PHs, with the degree of hydrolysis not necessarily correlating with the concentration of specific amino acids (Table 2). For example, H2 contained 3.2-, 2.1-, and 1.7-fold higher concentrations of L-asparagine, L-lysine, and L-glycine, respectively, than H1, although H1 had a 1.25-fold higher degree of hydrolysis than H2. Differences in all amino acid concentrations between H1 and H3 were below 1.2-fold, consistent with their differences in hydrolysis degree. There were 54 di- and tripeptides detected with different abundances (Table 2). The most numerous (7) were arginine-containing dipeptides, with arginine-isoleucine being most abundant in all three PHs, with H1 containing the highest values.

Table 2. Degree of hydrolysis (averages of n = 4 ± standard error are shown), concentration of amino acids, and non-targeted peptide profiles (normalized data) measured in protein hydrolysates (H1, H2, and H3) used in the experiment. Different letters above columns represent statistically significant differences between treatments (One-Way ANOVA and LSD post hoc test at $p < 0.05$). <LLOQ, lower limit of quantification, n.d., not detected.

		H1	H2	H3
Degree of hydrolysis		88.8 ± 0.51 [a]	71.0 ± 0.38 [c]	77.4 ± 0.25 [b]
Amino acids (mg L^{-1})	L-glycine	7.95	13.8	18.1
	4-amino butanoic acid	137	64	42.9
	L-proline	<LLOQ	1.39	0.611
	L-threonine	<LLOQ	<LLOQ	<LLOQ
	trans-4-hydroxy-L-proline	4.43	4.37	3.22
	L-leucine	22	21.2	17.4
	L-asparagine	9.3	29.9	32.2
	L-glutamine	64.7	78	71
	L-lysine	6.86	14.1	11.2
	L-methionine	8.02	5.32	5.21
	L-phenylalanine	28.1	24	20.9
	L-cysteic acid	<LLOQ	<LLOQ	<LLOQ
	L-arginine	24.5	40.7	31.9
	L-tyrosine	21.9	21.8	21
	L-serine	15.2	22.5	20.7
	L-valine	20.8	20.5	14
	L-glutamic acid	2.5	3.51	8.59
Compounds (abundance)	alanine—glutamine	365	348	150
	alanine—leucine	138	116	47.8
	alanine—methionine	46.9	27.8	9.39
	alanine—phenylalanine	144	86.5	41.3
	arginine—alanine	80.2	22.7	25.2
	arginine—glycine	16.2	8.98	7.87
	arginine—isoleucine	24,412	7348	8406
	arginine—methionine	1613	542	287
	arginine—proline	1.72	4.85	1.01
	arginine—serine	10.4	2.53	2.92
	arginine—valine	1465	561	477
	asparagine—leucine	557	268	114
	glutamine—glutamine	151	164	54
	glycine—leucine	847	460	126
	glycine—leucine	752	450	347
	isoleucine—glutamic acid	49	78	85

Table 2. *Cont.*

		H1	H2	H3
Compounds (abundance)	isoleucine—leucine	362	359	211
	isoleucine—proline	353	232	56
	leucine—asparagine	226	133	100
	leucine—leucine—tryptophan	63	60	33
	leucine—phenylalanine	409	250	205
	lysine—leucine	1398	405	125
	3-methyl-histidine	1.1	n.d.	1.37
	methyl-lysine	n.d.	n.d.	n.d.
	methionine—leucine	22.9	32.6	5.4
	methionine—phenylalanine	45.6	33.2	15.2
	phenylalanine—alanine—leucine	81.6	29.6	12.6
	phenylalanine—glycine	342	194	153
	phenylalanine—isoleucine	159	74	38
	phenylalanine—phenylalanine	20.6	6.7	5.5
	proline—glutamine	207	404	28
	proline—histidine	2.53	55.9	28.1
	proline—valine	133	392	26
	serine—leucine	139	68.9	25.4
	serine—phenylalanine	124	60.5	19
	threonine—leucine	27.5	34.9	24.5
	threonine—phenylalanine	18.2	13.7	13.9
	tryptophan—leucine	61.5	39	41
	tyrosine—arginine	1639	322	196
	tyrosine—isoleucine	18.9	15.4	5.26
	valine—glutamine	202	84	51
	valine—isoleucine	166	244	127
	5-hydroxytryptophano	236	346	397
	pyroglutamyl—isoleucine	272	326	96
	glycine—phenylalanine	162	138	95
	serine—isoleucine	160	52.6	13.5
	arginine—leucine	785	328	465
	leucine—leucine	92	124	70
	threonine—isoleucine	60.6	46.1	46.8
	alanine—isoleucine	54.8	60	23.1
	glycine—valine	32.1	61.6	24.1
	glycine—glutamine	150	109	110
	threonine—glutamine	128	103	86.7
	serine—asparagine	121	109	95.2

By contrast, there were minimal differences in element composition between the three PHs, with H3 tending to have the lowest values, especially of micronutrients (Table 3).

Table 3. Concentrations of elements in protein hydrolysates (H1, H2, and H3) used in the experiment. Averages (n = 4) ± standard errors are shown. Different letters above columns represent statistically significant differences between treatments (One-Way ANOVA and LSD post hoc test at $p < 0.05$).

		H1			H2			H3		
mg L^{-1}	Mg	13.94	±	0.421 ^{a}	14.7	±	0.245 ^{a}	13.2	±	0.610 ^{a}
	K	2.43	±	0.058 ^{b}	2.66	±	0.0129 ^{a}	1.51	±	0.100 ^{c}
	Ca	42.54	±	0.896 ^{a}	42.8	±	0.525 ^{a}	42.7	±	0.407 ^{a}
	Zn	1.83	±	0.099 ^{a}	0.955	±	0.025 ^{b}	0.481	±	0.021 ^{c}
µg L^{-1}	Mn	6.99	±	0.690 ^{ab}	8.02	±	0.209 ^{a}	4.83	±	0.135 ^{b}

Table 3. *Cont.*

	H1			H2			H3		
Fe	63.1	±	5.56 ^{b}	90.3	±	6.06 ^{a}	42.2	±	1.24 ^{c}
Cu	77.3	±	5.06 ^{b}	102	±	3.59 ^{a}	28.6	±	2.64 ^{c}
B	7.26	±	0.678 ^{a}	4.56	±	0.754 ^{b}	3.78	±	0.859 ^{b}

3.1. Shoot and Root Growth and Leaf Reflectance

Shoot and root growth and leaf reflectance were assessed in the one-year-old olive seedlings sprayed with the three PHs under control conditions. Olive seedlings did not show any toxicity or deficiency symptoms throughout the experiment (Figure 1a). Shoot growth (height) was significantly enhanced in the H2 and H3 treatments by 20–30% ($p < 0.05$) compared to the C or H1 treatments (Figure 1a). Among the reflectance indices measured, significant treatment effects were observed for the Chlorophyll-Normalized Difference Vegetation Index (CNDVI), greenness index (GI), photochemical reflectance index (PRI), and structure insensitive pigment index (SIPI), and not for the water band index (WBI) and plant senescence reflectance index (PSRI; Figure 1a). Control- and H2-treated plants had higher CNDVI values than H1- and H3-treated plants, while PRI was significantly higher in the H2 treatment compared to other treatments (Figure 1a). The GI and SIPI showed contrasting trends: GI was the lowest, while SIPI was the highest in C plants compared to other treatments (Figure 1a).

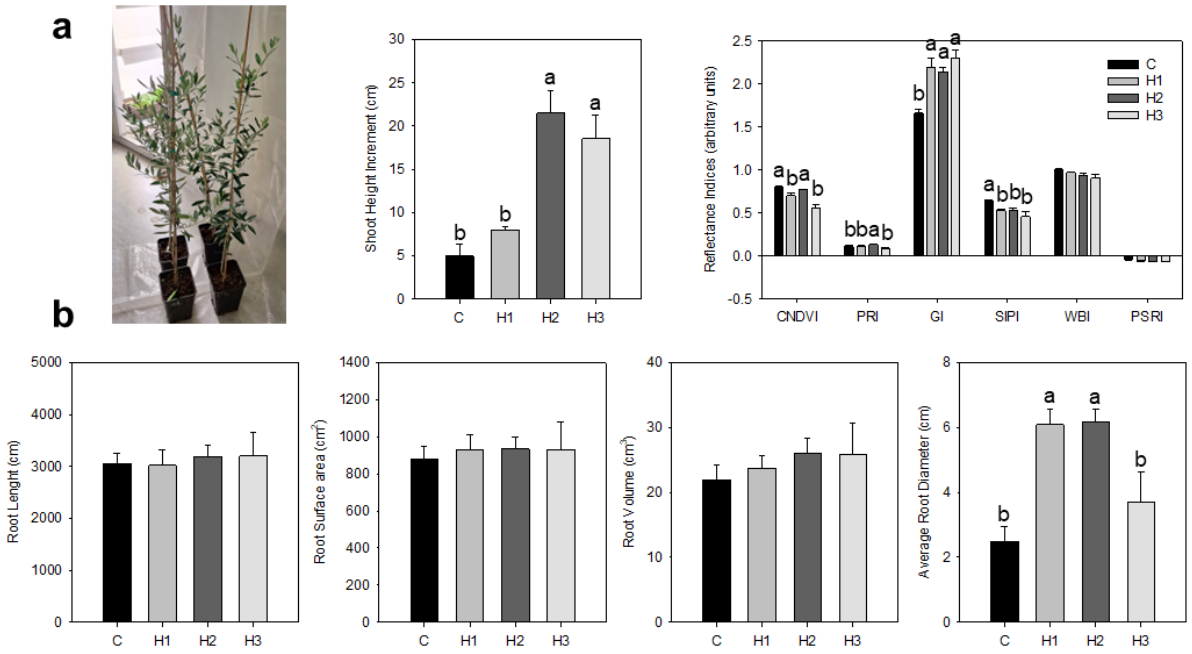

Figure 1. Shoot growth and reflectance indices (**a**) and root growth parameters (**b**) in one-year-old seedlings of olive (*Olea europaea* cv. *Leccino*) to which water and a wetting agent (control, C) or additional protein hydrolysates (H1 − H3, detailed amino acid, peptide and element composition is provided in Tables 2 and 3) were foliarly applied six times in eight-day intervals under controlled conditions. Means (n = 4) ± standard errors are shown. Different letters indicate significant differences according to main-effects ANOVA with Fisher's LSD test ($p < 0.05$). Reflectance indices are defined in Table 1.

In contrast to root length, root surface area, and root volume, the average root diameter was significantly affected by treatments: it was higher in H1- and H2-treated plants than in C and H3-treated plants (Figure 1b).

3.2. Element Composition of Olive Organs

At harvest, young and old leaves were separated in addition to sampling stems and roots for mineral element composition of one-year olive seedlings sprayed with three different PHs under controlled conditions. There were apparent differences in mineral element concentrations between olive organs: all micronutrients analyzed, except B, were higher in roots than in other organs, Mg, Ca, and B concentrations were higher in old leaves than in other organs, and K concentrations were higher in young leaves than in other organs (Figure 2).

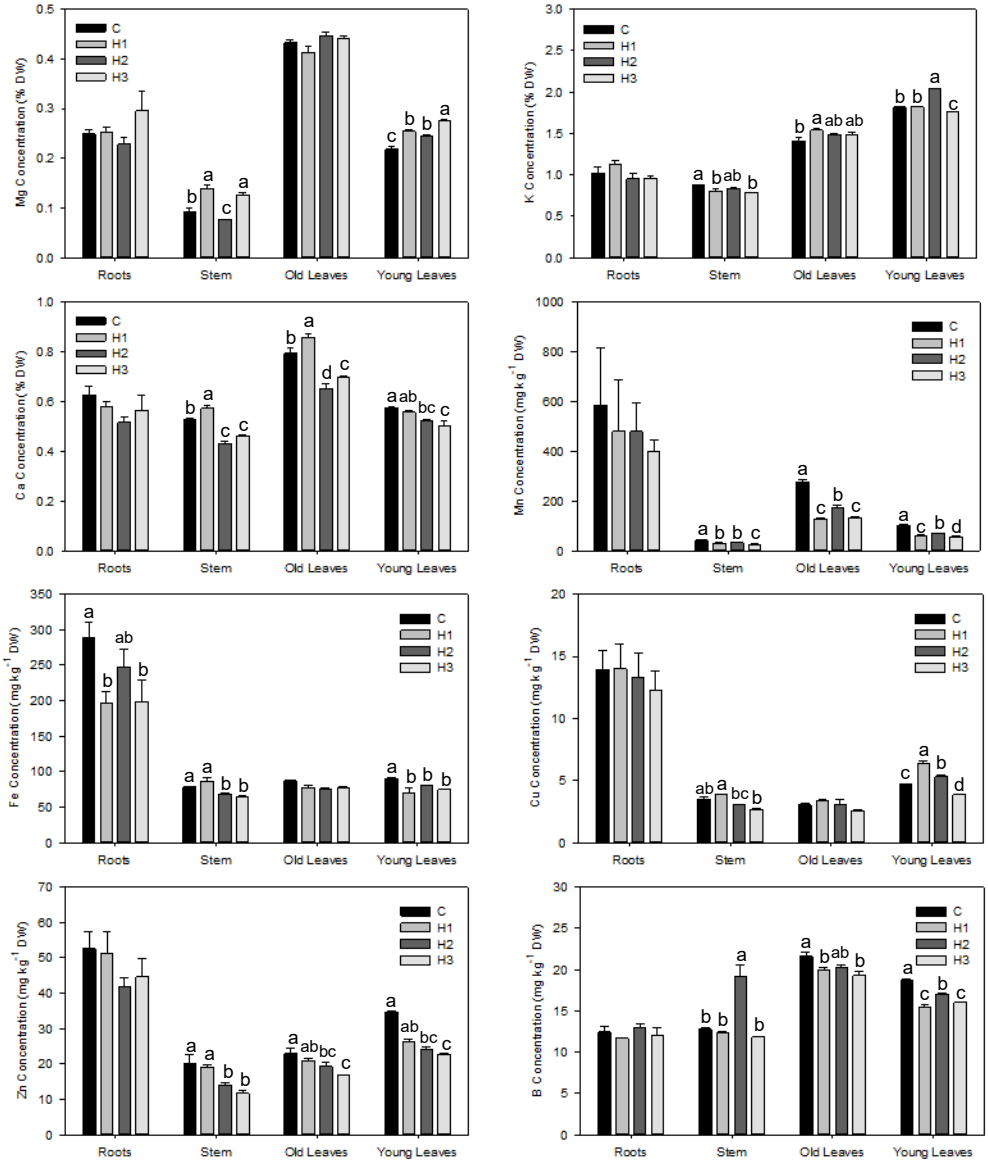

Figure 2. Bulk concentrations of magnesium (Mg), potassium (K), calcium (Ca), iron (Fe), manganese (Mn), copper (Cu), zinc (Zn) and boron (B) in roots, stem, young, and old leaves of one-year-old seedlings of olive (*Olea europaea* cv. *Leccino*) to which water and a wetting agent (control, C) or additional protein hydrolysates (H1 − H3, detailed amino acid, peptide and element composition is provided in Tables 2 and 3) were foliarly applied six times in eight-day intervals under controlled conditions. Averages (n = 4) ± standard errors are shown. Different letters indicate significant differences according to main-effects ANOVA with Fisher's LSD test or rank-based main-effects ANOVA with Bonferroni-adjusted pairwise comparisons ($p < 0.05$). DW, dry weight.

In roots, the only significant treatment effects were observed for Fe concentrations: C plants had the highest concentrations, H1- and H3-treated plants had significantly lower concentrations, and H2-treated plants had intermediate values (Figure 2).

By contrast, there was a significant effect of treatments on all mineral elements in the stem; however, no general trend could be found (Figure 2). Magnesium concentrations were the highest in H1 and H3-treated plants, followed by C plants and finally by H2-treated plants. Potassium concentrations were the highest in C plants and declined in the treatments, except in H2-treated plants, where they were intermediate. Calcium concentrations in stems were the highest in H1-treated plants, followed by C plants and finally by H2 and H3-treated plants. Manganese concentrations in the stems were highest in C plants and declined in H1- and H2-treated plants and in H3-treated plants. There was a common trend in Fe and Zn concentrations in the stems, with C plants and H1-treated plants having higher concentrations than H2 and H3-treated plants. A significant increase in stem B concentrations was observed in H2-treated plants.

In old leaves, Mg, Fe, and Cu concentrations were not affected by treatments (Figure 2). Similarly to the results in the stems, no general trend in PH effects on the concentration of the analyzed mineral elements in old leaves could be deduced. H1-treated plants had significantly higher K concentrations in their old leaves than C plants, but not higher than H2- and H3-treated plants, while Ca concentrations in old leaves were the highest in H1-treated plants, followed by C plants, and were significantly lower in H2- and H3-treated plants. Manganese, Zn, and B concentrations were higher in the old leaves of C plants than in those of the other two treatments (Figure 2).

In young leaves, all measured mineral nutrients were significantly affected by the treatments (Figure 2). A trend of increasing concentrations from C plants to H3-treated plants can be observed for Mg concentrations and a decrease for Ca, Mn, Fe, Zn, and B concentrations, whereas H2-treated plants had significantly higher K concentrations and H1-treated plants had higher Cu concentrations than plants in other treatments (Figure 2).

3.3. Element Composition of Leaf Tissues

While bulk element concentrations depict the general nutrition status of the one-year old olive seedlings sprayed with three PHs under control conditions, there may be tissue-specific changes in the leaf tissues. Therefore, mineral element localization analyses were used to capture responses at the tissue level in leaves. Phosphorus, S, Cl, K, Ca, Mn, Fe, Cu, and Zn were detected, and their tissue allocation in olive leaf cross sections was captured (Figures 3 and 4). From quantitative distribution images, concentrations in the whole section (W), lower epidermis (LE), upper epidermis (UE), palisade mesophyll (PM), and spongy mesophyll (SM) were measured. For P, S, Cl, K, and Ca, concentrations are given as weight %, whereas for Mn, Fe, Cu, and Zn, concentrations are given as mg kg^{-1} of dry weight.

Of all mineral elements analyzed, P was the only element for which there was a significant effect of treatments observed in all leaf tissues: there was significantly less P in W, PM, and SM in H1- and H3-treated plants than in C and H2-treated plants, whereas in epidermises there was negative effect on P concentrations in all three treatments compared to C (Figure 3). An opposite trend, although not significant in all instances, was observed for Cl concentrations: higher values were found in the leaf tissues of H1- and/or H3-treated plants than in C and/or H1-treated plants (Figure 3). An apparent decrease in S, K, and Ca concentrations was observed in the LE of leaves from H2- and H3-treated plants compared to C and H1-treated plants (Figure 3). This observation was not mirrored in UE. Potassium concentrations increased in SM, with the highest values observed in the H2 and H3 treatments, which were significantly higher than in the untreated C plants.

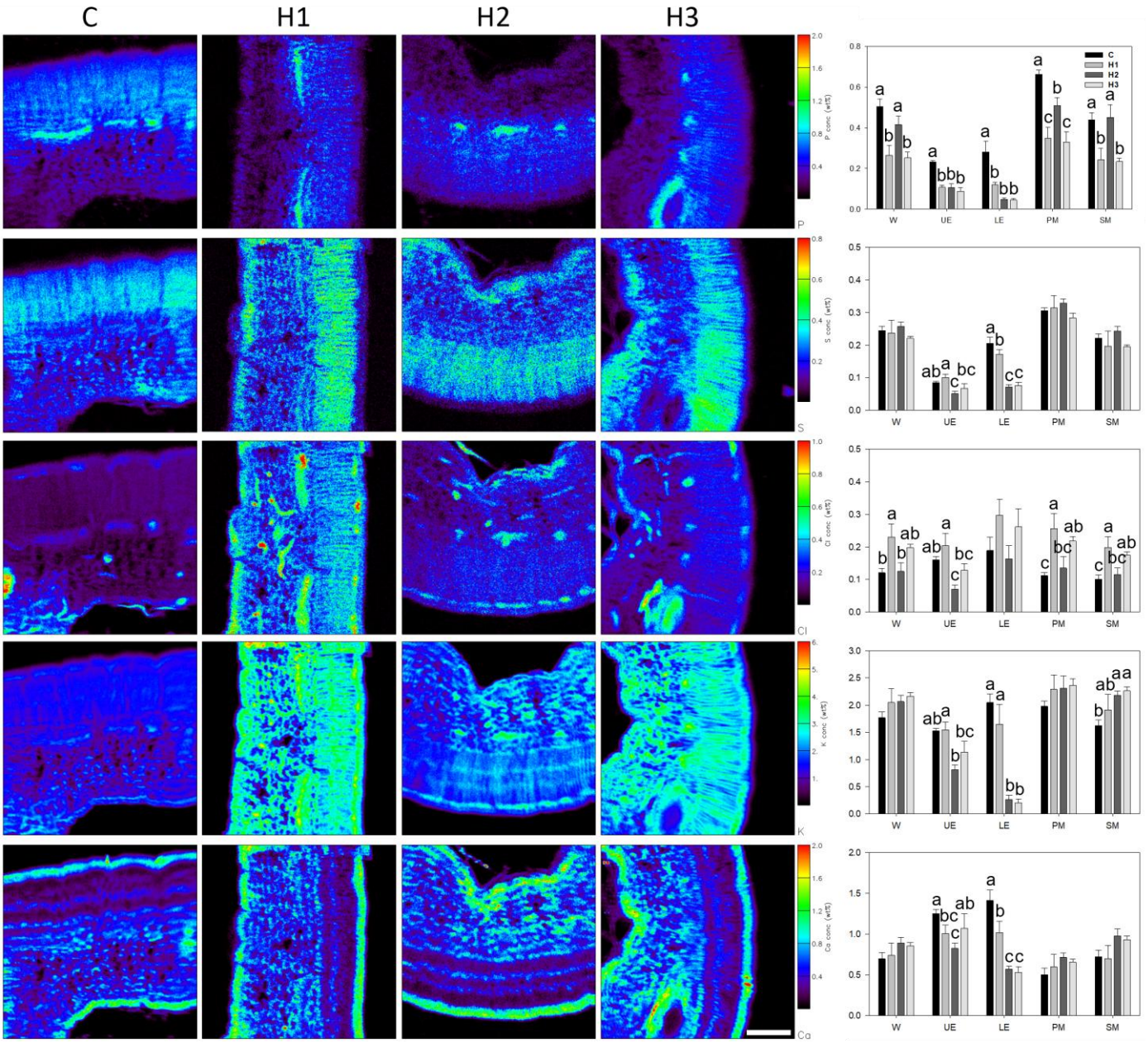

Figure 3. Representative distribution maps and tissue-specific concentrations (in % dry weight) of phosphorus (P), sulphur (S), chlorine (Cl), potassium (K) and calcium (Ca) in the cross-sections of leaves of one-year-old seedlings of olive (*Olea europaea* cv. *Leccino*) to which water and a wetting agent (control, C) or additional protein hydrolysates (H1–H3, detailed amino acid, peptide and element composition is provided in Tables 2 and 3) were foliarly applied six times in eight-day intervals under controlled conditions. Bar charts represent averages (n = 4) ± standard errors. W, whole section; UE, upper epidermis; LE, lower epidermis; PM, palisade mesophyll; SM, spongy mesophyll. Different letters indicate significant differences according to main-effects ANOVA with Fisher's LSD test or rank-based main-effects ANOVA with Bonferroni-adjusted pairwise comparisons ($p < 0.05$). Scale bar indicates 100 µm and is the same for all maps.

The allocation of micronutrients was only significantly affected by treatments in the epidermises (Figure 4). There was an apparent trend of C plants having the highest concentrations of Mn and Cu in UE and of C and H1-treated plants having higher Cu in LE. Also, C plants exhibited higher Fe concentrations than H2 plants in both epidermises. Manganese and Zn concentrations decreased from C plants toward H2- and/or H3-treated plants (Figure 4).

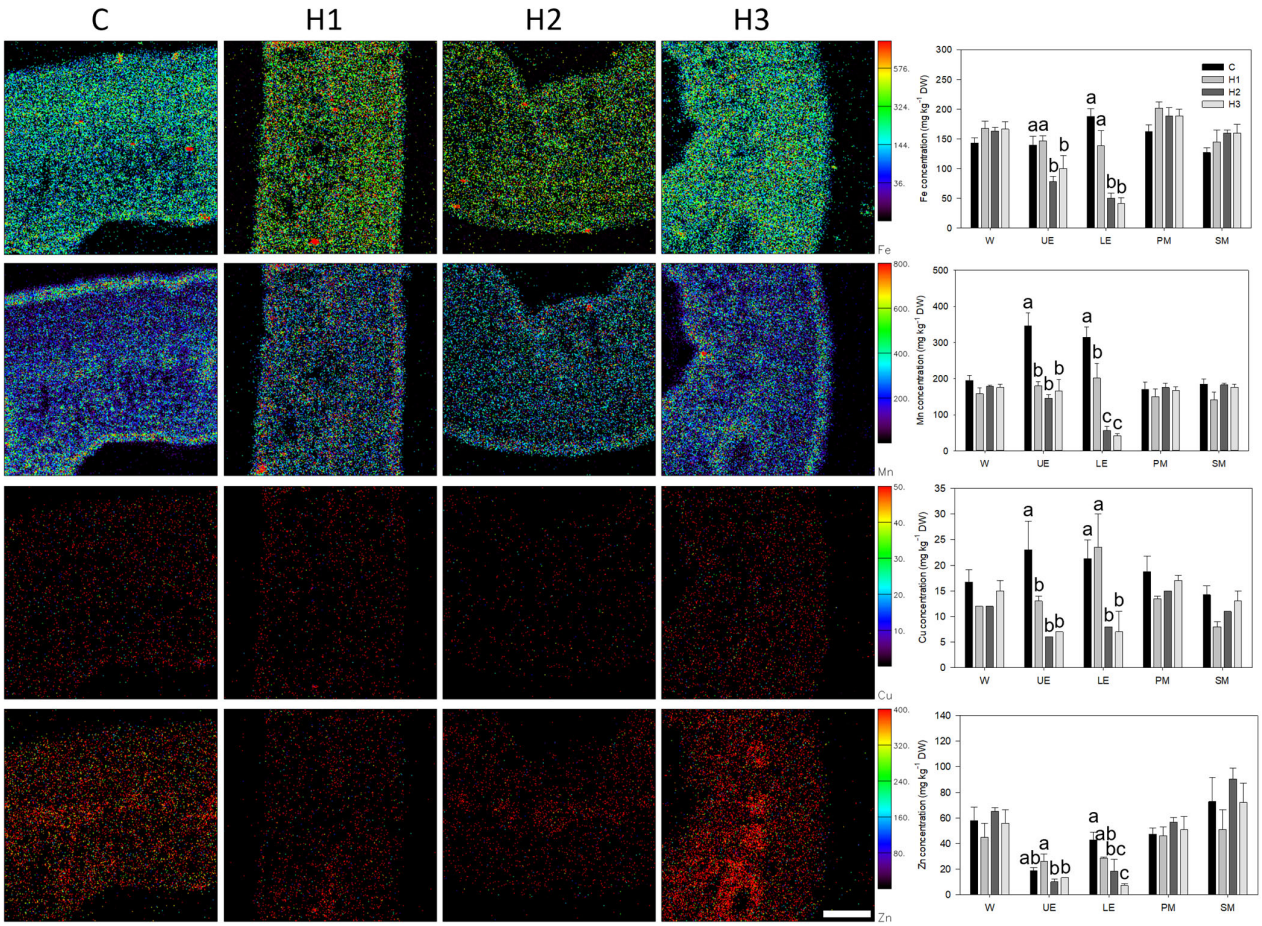

Figure 4. Representative distribution maps and tissue-specific concentrations (in mg kg^{-1} dry weight) of iron (Fe), manganese (Mn), copper (Cu) and zinc (Zn) in the cross-sections of leaves of one-year-old seedlings of olive (*Olea europaea* cv. *Leccino*) to which water and a wetting agent (control, C) or additional protein hydrolysates (H1 − H3, detailed amino acid, peptide and element composition is provided in Tables 2 and 3) were foliarly applied six times in eight-day intervals under controlled conditions. Bar charts represent averages (n = 4) ± standard errors. W, whole section; UE, upper epidermis; LE, lower epidermis; PM, palisade mesophyll; SM, spongy mesophyll. Different letters indicate significant differences according to main-effects ANOVA with Fisher's LSD test or rank-based main-effects ANOVA with Bonferroni-adjusted pairwise comparisons ($p < 0.05$). Scale bar indicates 100 µm and is the same for all maps.

4. Discussion

4.1. Protein Hydrolysates

The biological and functional properties of PHs are strongly influenced by factors such as degree of hydrolysis, enzyme specificity, and protein substrate type [29]. Using a single protein isolate from pumpkin seed cake, a protein-rich by-product of pumpkin oil production [30] popular in the region, and three different enzyme combinations, we obtained three mixtures. They comprised different amino acid compositions with large di and tripeptide diversity (Table 2) and low element concentrations (Table 3). Enzymatic hydrolysis was used because it is a gentle process for preparing food PHs with fewer undesirable side effects. Three different enzymes were used. Alcalase is an endopeptidase that cleaves peptide bonds at the C-terminal amino acid and was the most effective, resulting in the highest degree of hydrolysis. In contrast, Flavourzyme is both an endo- and exopeptidase that cleaves at the N-terminal of peptide chains. Protana (also known as Protamex) is a broad-spectrum endoprotease that hydrolyses proteins into smaller peptides and amino acids. Alcalase tends to produce smaller peptides more readily than Protana, which aligns

with studies on Whey Protein Isolate, soybean, and fish protein [31–33]. This behavior can be attributed to the type of enzyme. Alcalase has greater activity than Protana due to its higher specificity for serine residues and its endoproteolytic activity [34], and is known to produce mainly small, hydrophobic peptides [35].

4.2. Effects of Protein Hydrolysates on Growth and Leaf Reflectance Composition in One-Year Old Olive Seedlings

Foliar application of the PHs was expected to elicit local and systemic responses in one-year-old olive seedlings. The increased shoot height in the H2 and H3 treatments compared to the C and H1 treatments was accompanied by the H2 treatment showing more favorable reflectance indices (Figure 1a), indicating that the H2 treatment had the most significant effect on above-ground plant fitness. These responses are consistent with improved chlorophyll status, enhanced photosynthetic performance, and reduced stress intensity [36,37] in H2-treated plants compared to other treatments. Moreover, the average root diameter was higher in plants from the H2 treatment than in plants from the C (Figure 1b), corroborating conclusions from the above-ground observations. Because PH mixtures were used in this experiment, only limited mechanistic inferences are possible. Because element concentrations in the PH mixtures were so low (Table 3) and there was little meaningful correlation with bulk element concentrations, the amino acid and or di and tripeptide composition of the PHs was examined for pivotal candidates, considering observed effects individually. For example, positive shoot height effects observed for H2 and H3 may be a consequence of their 3.22-fold and 3.47-fold higher concentrations of L-asparagine than in the H1 mixture, respectively. This N-containing amino acid has recently been reported to have a biostimulant effect on leaf area in *Arabidopsis thaliana* [38], but no mechanistic interaction was proposed. The superiority of the H2 mixture over both H1 and H3 mixtures in reflectance indices (Figure 1) may be associated with a 2.3-fold higher L-proline concentration in H2 over H3 (in the H1 mixture, no L-proline was detected), despite low absolute levels. Proline is a well-known compatible osmolyte and potential reactive oxygen species (ROS) scavenger [39], and its exogenous application in numerous fruit trees has shown significant enhanced fruit qualities [40]. However, given the low absolute concentrations detected, its quantitative contribution to the observed responses remains uncertain. A further amino acid candidate for the observed differences in reflectance indices may be the higher L-arginine concentration found in H2 compared to H3 and H1 mixtures, as arginine is a key N-containing amino acid [41] and has been shown to alleviate the reduction in photosynthesis and antioxidant activity induced by drought stress in maize seedlings [42]. Furthermore, in N-deficient apple, hydroponically supplied arginine was shown to promote photosynthesis capacity, alter amino acid metabolism, and improve tolerance to N deficiency, possibly through improving the uptake and translocation of N, P, and K [43]. In addition, the fourth amino acid candidate is L-lysine, which has been typically applied as a biostimulant in a complex with Zn, resulting in better photosynthesis efficiency in water-stressed maize [44] or with Fe, boosting photosynthetic pigments in cadmium-stressed canola [45]. Less is known about the effects of L-lysine in woody species, including olive [46].

The long-distance effect (i.e., root growth parameters) of treatments was only measurable in the average root diameter, which was higher in the H1 and H2 treatments compared to the C and H3 treatments (Figure 1b). One of the amino acids, the concentrations of which were higher in the H1 and H2 mixtures than in the H3 mixture, was L-valine (Table 2). Exogenous valine has been shown to promote root growth and to inhibit the shoot growth of peach seedlings [47]. The shoot growth inhibition was prevented in these peach seedlings if isoleucine was sprayed. While the L-isoleucine was not detected in the PHs, there were 11 isoleucine-containing dipeptides found, and arginine-isoleucine was most abundant of

all, with the H1 mixture containing the highest values (Table 2). It seems that isoleucine in dipeptide form does not have the same effect as exogenously applied isoleucine, as in H1-treated olive seedlings, shoot growth did not reach that of H2- and H3-treated plants. These observations clearly imply that tailoring optimized PH combinations will be very challenging and will probably be species-specific.

So far, we have examined only amino acids whose concentrations were higher in the H2 mixture compared to the H1 or H3 mixtures. However, it may as well be that the concentration of an individual amino acid is not responsible for an observed effect, but rather that their combination(s) is. While experiments with individual amino acids or defined mixtures would be required to draw firm mechanistic conclusions, our aim is to design an agronomically acceptable biostimulant from an agronomic waste product, valorizing it and enabling its use in sustainable agronomic practice.

4.3. Effects of Protein Hydrolysates on Mineral Element Composition in One-Year Old Olive Seedlings

Young leaves were defined as those that developed during the experiment; therefore, we assumed they had been treated to a lesser extent than older leaves. In addition, young (developing) leaves are considered a mineral sink for elements, particularly those with greater phloem mobility, such as K, P, Mg, and Zn [48]. As there is a continuous shift in sink/source relationship within a plant, the element composition of any of the plant parts measured at a selected time point is a consequence of several physiological processes, including uptake, storage, and (re)translocation, in line with the current demands of the tissue. Additional external applications of mineral elements that cannot be traced in vivo further complicate the picture. In this study, the PHs did not contain large quantities of mineral elements (Table 3); therefore, extensive increases in total element concentrations were not expected to be due to the foliar application itself. Indeed, only occasionally did the concentration of the measured elements in any of the plant parts increase (Figure 2). Rather, changes in mineral composition were an indirect consequence of amino acid and di- and tripeptide activity as signaling molecules, or of their interactions with physiological processes linked to mineral nutrition. One example of such an interaction reports that exogenously applied valine inhibited the growth of peach tree shoots by regulating the balance between sucrose non-fermenting-1-related protein kinase and target of rapamycin kinase [47]. The latter plays a key role in responses to starvation and induces autophagy in plants [49], a process involved in responses to mineral deficiency and/or senescence.

In olive seedlings, the pH treatments did not change the overall predominant allocation of mineral elements to a specific plant organ. All micronutrients analyzed, except B, were higher in the roots than in other organs. Mg, Ca, and B concentrations were higher in old leaves than in other organs, whereas K concentrations were higher in young leaves than in other organs (Figure 2). At least observations of differences between old and young leaves (concentrations in stems and roots are rarely reported, as their removal from slow-growing trees, such as olives, means the termination of the experiment) can be confirmed in the literature [50,51]. The robustness of these organ-level allocation patterns varied among elements and tissues, as indicated by the observed power analysis (Supplementary Table S1). In particular, K allocation to young leaves was supported by high statistical power, whereas the root accumulation of micronutrients was associated with lower power and should therefore be interpreted cautiously. Looking at PH-specific effects on bulk mineral elements concentrations reveals that a similar distinctive beneficial effect was observed for the growth and leaf reflectance indices for the H2 treatment in comparison to C plants, which was observed for K concentration in young leaves and B concentration in the stems (Figure 2). Increases in K concentrations after foliar application of PHs were reported in pea plants (*Pisum sativum*) in a field experiment [52], an increase in K channel

expression when PHs were added to the nutrient solution of growing tomato plants [53] and under saline stress conditions, plants treated with biostimulants showed higher levels of K and proline compared to untreated controls [8]. All these reports are in line with our observation, but only for the H2 treatment of young leaves and the H1 treatment of old leaves. Within leaf tissues, K concentrations in SM were higher in H2-treatment (and in H3 treatment) than in C plants (Figure 3). Interestingly, these two treatments had significantly less K in LE than C and H1-treated plants, which suggests a redistribution of K from LE towards the SM if high short-distance transport of K resembles the high long-distance phloem mobility of K [48]. Such redistribution likely reflects more vigorous metabolic and osmotic activity in the SM of H2- and H3-treated plants, which is consistent with the physiological role of K in supporting cell expansion, turgor maintenance, and photosynthetic performance during active growth [54–57], which was clearly observed in olive seedlings treated with the H2 and H3 mixtures (Figure 1). However, while the reduction in K in the LE was supported by high statistical power, the increase in the SM was associated with moderate power and should therefore be interpreted with appropriate restraint.

Nevertheless, there were instances when H2-treated plants had significantly lower concentrations than C plants (e.g., in the stem, all elements except B) or when this was observed in conjunction with H3-treated plants (e.g., in old and young leaves for Ca, and young leaves for Fe), making robust mechanistic interpretation difficult. In general, it seems that, for all elements, LE was mainly negatively affected by PH treatments, particularly by H2 and H3 treatments, as consistently lower concentrations of all elements, except for Cl, were observed in C-treated plants (Figures 3 and 4). Again, the higher L-arginine and L-proline concentration in H2 and H3 mixtures compared to the H1 mixture could play a synergistic role in element relocation from epidermis to mesophyll. Arginine is a precursor of polyamines, a class of phytohormones that regulate the voltage-dependent inward K^+ channel in the plasma membrane of guard cells and induce stomatal closure [58], thereby limiting transpiration and hence the delivery of essential elements to the leaves. Local element deficiency may be remedied by the redistribution of those elements from the epidermis to the metabolically active mesophyll. Polyamines can increase ROS levels in guard cells [59], which can be scavenged by the applied L-proline, thereby maintaining the physiological stability of olive leaves. However, since polyamine levels and stomatal parameters were not measured in this study, these interpretations remain hypothetical and are presented as possible explanatory mechanisms.

Peculiar was a contrasting treatment response in mesophyll concentrations of P and Cl (Figure 3), with P concentrations higher in C and H2-treated plants than in H1- and H3-treated plants. In comparison, Cl concentrations were higher in H1- and/or H3-treated plants than in C plants. While treatment-related differences observed in the stem and for Ca and Fe in old and young leaves were generally supported by high observed statistical power, the contrasting Cl mesophyll responses and LE effects were associated with moderate to low power, respectively (Supplementary Table S1), limiting the interpretability of these tissue-specific patterns. Although the uptake of P and Cl by roots was reported to be antagonistic [60,61], their tissue-specific allocation in leaves and the effects of treatments should be investigated further.

5. Conclusions

The foliar application of PHs from valorized agronomic waste (pumpkin seed cake), particularly the H2 and H3 mixtures, to one-year-old olive seedlings under controlled conditions resulted in improved shoot growth and reflectance index compared with untreated C plants, reflecting improvement in photosynthetic activity. Considering also the element composition of plant parts, the H2 mixture appears the most promising foliar

PHs treatment, suitable for improving nutrient uptake and photosynthetic performance of olives without significantly affecting bulk ionome homeostasis. At the leaf tissue level, conspicuous redistribution of elements from epidermis to mesophyll was observed, presumably to support increased metabolic demands that sustained increased shoot growth. Arguably, these observed effects could be attributed to the amino acid profile of the H2 mixture, which has the highest concentration of L-proline, L-arginine, and L-lysine among the three PHs mixtures, and a higher L-asparagine concentration than the H1 mixture. Further mechanistic experiments are required to resolve modes of action of PHs and/or individual amino acids, and a field experiment to corroborate the beneficial physiological effects observed in this experiment and to evaluate agronomic effects, particularly the potential benefits to yield and olive oil quality.

Supplementary Materials: The following supporting information can be downloaded at https://www.mdpi.com/article/10.3390/horticulturae12020151/s1, Table S1: Post hoc power analysis of treatment effects for organ-level and tissue-specific elemental variables analyzed using a randomized complete block design.

Author Contributions: Conceptualization: I.P., P.P., L.P., and M.P.P.; validation and formal analysis: P.Ž., M.Š., M.P.P., P.P., P.V., M.A., L.P., M.F., I.D., and H.P.; investigation: I.P., I.D., L.P., M.A., and M.P.P.; resources: I.P., L.P., S.G.B., P.Ž., and P.P.; data curation: I.P., P.P., H.P., P.V., P.Ž., M.F., L.P., S.G.B., T.K., M.Š., and M.P.P.; writing—original draft preparation: I.P., L.P., and M.P.P.; writing—review and editing: I.P., P.P., T.K., and M.P.P.; visualization: P.P. and M.P.P.; supervision: I.P. and P.P.; project administration: I.P., P.P., and M.P.P.; funding acquisition: I.P. and P.P. All authors have read and agreed to the published version of the manuscript.

Funding: This work was funded by the Croatian Science Foundation (CSF (HRZZ)) and the Slovenian Research and Innovation Agency (ARIS) under the WEAVE initiative bilateral project HRZZ- IP-2022-10-8305 and N4-0346 (PROGRESS) and through core ARIS funding (P1-0212). Access to micro-PIXE facility (ID 34772) was enabled by the European Union as part of the Horizon Europe call HORIZON-INFRA-2021-SERV-01 under grant agreement number 101058414 and co-funded by UK Research and Innovation (UKRI) under the UK government's Horizon Europe funding guarantee (grant number 10039728) and by the Swiss State Secretariat for Education, Research and Innovation (SERI) under contract number 22.00187. Views and opinions expressed are, however, those of the author(s) only and do not necessarily reflect those of the European Union, the UK Science and Technology Facilities Council, or the Swiss State Secretariat for Education, Research and Innovation (SERI). Neither the European Union nor the granting authorities can be held responsible for them. The authors acknowledge the financial support from the Slovenian Research and Innovation Agency (ARIS), research core funding No. P1-0034. In addition, the work of PhD student M.P.P. was supported by the "Young researchers career development project-training of doctoral students" program under the CSF project no. HRZZ-DOK-2021-02-5517 and HRZZ-MOBDOK-2023-3103, and the work of PhD student I.D. was supported by the "Young researchers career development project-training of doctoral students" program under the CSF project no. HRZZ DOK-NPOO-2023-10-1951.

Data Availability Statement: The raw data supporting the conclusions of this article will be made available by the authors on request.

Conflicts of Interest: The authors declare no conflicts of interest.

References

1. Polić Pasković, M.; Herak Ćustić, M.; Lukić, I.; Marcelić, Š.; Žurga, P.; Vidović, N.; Major, N.; Goreta Ban, S.; Pecina, M.; Ražov, J.; et al. Foliar nutrition strategies for enhancing phenolic and amino acid content in olive leaves. *Plants* **2024**, *13*, 3514. [CrossRef] [PubMed]
2. Martins, S.; Pereira, S.; Dinis, L.-T.; Brito, C. Enhancing olive cultivation resilience: Sustainable long-term and short-term adaptation strategies to alleviate climate change impacts. *Horticulturae* **2024**, *10*, 1066. [CrossRef]

3. Saifi, R.; Kokiçi, H.; Saifi, H.; Akça, I.; Benabdelkader, M.; Xhemali, B.; Çota, E.; Hadjeb, A. Does climate change heighten the risk of *Xylella fastidiosa* infection? In *Plant Quarantine Challenges Under Climate Change Anxiety*; Springer: Cham, Switzerland, 2024; pp. 331–358. [CrossRef]
4. Fernández-Escobar, R. Olive nutritional status and tolerance to biotic and abiotic stresses. *Front. Plant Sci.* **2019**, *10*, 1151. [CrossRef] [PubMed]
5. Calvo, P.; Nelson, L.; Kloepper, J.W. Agricultural uses of plant biostimulants. *Plant Soil* **2014**, *383*, 3–41. [CrossRef]
6. Carillo, P.; Avice, J.-S.; Vasconcelos, M.W.; du Jardin, P.; Brown, P.H. Biostimulants in Agriculture: Editorial. *Physiol. Plant.* **2025**, *177*, e70046. [CrossRef]
7. Du Jardin, P. Plant biostimulants: Definition, concept, main categories and regulation. *Sci. Hortic.* **2015**, *196*, 3–14. [CrossRef]
8. Colla, G.; Hoagland, L.; Ruzzi, M.; Cardarelli, M.; Bonini, P.; Canaguier, R.; Rouphael, Y. Biostimulant action of protein hydrolysates: Unravelling their effects on plant physiology and microbiome. *Front. Plant Sci.* **2017**, *8*, 2202. [CrossRef]
9. Tadayon, M.S.; Asgharzadeh, A.; Mousavi, S.M.; Saghafi, K. Synergistic effects of chemical and biochemical fertilisation on yield enhancement and oil quality optimisation in 'Zard' olive cultivars. *Front. Plant Sci.* **2025**, *16*, 1455921. [CrossRef]
10. Zipori, I.; Erel, R.; Yermiyahu, U.; Ben-Gal, A.; Dag, A. Sustainable management of olive orchard nutrition: A review. *Agriculture* **2020**, *10*, 11. [CrossRef]
11. Erel, R.; Dag, A.; Ben-Gal, A.; Schwartz, A.; Yermiyahu, U. Flowering and fruit set of olive trees in response to nitrogen, phosphorus, and potassium. *J. Am. Soc. Hortic. Sci.* **2008**, *133*, 639–647. [CrossRef]
12. Hawkesford, M.J.; Cakmak, I.; Coskun, D.; De Kok, L.J.; Lambers, H.; Schjoerring, J.K.; White, P.J. Functions of macronutrients. In *Marschner's Mineral Nutrition of Plants*; Academic Press: Cambridge, MA, USA, 2023; pp. 201–281.
13. Hasanuzzaman, M.; Bhuyan, M.H.M.B.; Nahar, K.; Hossain, M.S.; Mahmud, J.A.; Hossen, M.S.; Masud, A.A.C.; Moumita; Fujita, M. Potassium: A vital regulator of plant responses and tolerance to abiotic stresses. *Agronomy* **2018**, *8*, 31. [CrossRef]
14. Tariq, A.; Zeng, F.; Graciano, C.; Ullah, A.; Sadia, S.; Ahmed, Z.; Murtaza, G.; Ismoilov, K.; Zhang, Z. Regulation of metabolites by nutrients in plants. In *Plant Ionomics: Sensing, Signalling, and Regulation*; John Wiley & Sons Ltd.: Hoboken, NJ, USA, 2023; pp. 1–18. [CrossRef]
15. de Paiva Foletto-Felipe, M.; Abrahão, J.; Contesoto, I.C.; Ferro, A.P.; Grizza, L.H.E.; Menezes, P.V.M.C.; Wagner, A.L.S.; Seixas, F.A.V.; de Oliveira, M.A.S.; Tomazini, L.F.; et al. Inhibition of sulfur assimilation by S-benzyl-L-cysteine: Impacts on growth, photosynthesis, and leaf proteome of maize plants. *Plant Physiol. Biochem.* **2024**, *216*, 109173. [CrossRef]
16. Broadley, M.; Brown, P.; Cakmak, I.; Rengel, Z.; Zhao, F. Function of nutrients: Micronutrients. In *Marschner's Mineral Nutrition of Higher Plants*; Academic Press: Cambridge, MA, USA, 2023; pp. 191–248.
17. Perica, S.; Brown, P.H.; Connell, J.H.; Nyomora, A.M.; Dordas, C.; Hu, H.; Stangoulis, J. Foliar boron application improves flower fertility and fruit set of olive. *HortScience* **2001**, *36*, 714–716. [CrossRef]
18. Čakarević, J.; Šeregelj, V.; Tumbas Šaponjac, V.; Ćetković, G.; Čanadanović Brunet, J.; Popović, S.; Hadnađev Kostić, M.; Popović, L. Encapsulation of beetroot juice: A study on the application of pumpkin oil cake protein as new carrier agent. *J. Microencapsul.* **2020**, *37*, 121–133. [CrossRef] [PubMed]
19. Schymanski, E.L.; Jeon, J.; Gulde, R.; Fenner, K.; Ruff, M.; Singer, H.P.; Hollender, J. Identifying small molecules via high resolution mass spectrometry: Communicating confidence. *Environ. Sci. Technol.* **2014**, *48*, 2097–2098. [CrossRef]
20. Šelih, V.S.; Šala, M.; Drgan, V. Multi-element analysis of wines by ICP-MS and ICP-OES and their classification according to geographical origin in Slovenia. *Food Chem.* **2014**, *153*, 414–423. [CrossRef]
21. Pongrac, P.; Kelemen, M.; Vogel-Mikuš, K.; Vavpetič, P.; Pelicon, P.; Žurga, P.; Vidović, N.; Polić Pasković, M.; Smiljana, G.B.; Lukić, I.; et al. Tissue-specific calcium and magnesium allocation to explain differences in bulk concentration in leaves of one-year-old seedlings of two olive (*Olea europaea* L.) cultivars. *Plant Physiol. Biochem.* **2023**, *194*, 619–626. [CrossRef]
22. Pasković, I.; Pecina, M.; Bronić, J.; Perica, S.; Ban, D.; Ban, S.G.; Pošćić, F.; Palčić, I.; Herak Ćustić, M. Synthetic zeolite A as zinc and manganese fertilizer in calcareous soil. *Commun. Soil Sci. Plant Anal.* **2018**, *49*, 1072–1082. [CrossRef]
23. Ryan, C.G. Quantitative trace element imaging using PIXE and the nuclear microprobe. *Int. J. Imaging Syst. Technol.* **2000**, *11*, 219–230. [CrossRef]
24. Schindelin, J.; Arganda-Carreras, I.; Frise, E.; Kaynig, V.; Longair, M.; Pietzsch, T.; Preibisch, S.; Rueden, C.; Saalfeld, S.; Schmid, B.; et al. Fiji: An open-source platform for biological-image analysis. *Nat. Methods* **2012**, *9*, 676–682. [CrossRef]
25. R Core Team. *R: A Language and Environment for Statistical Computing*; R Foundation for Statistical Computing: Vienna, Austria, 2024. Available online: https://www.R-project.org/ (accessed on 4 January 2026).
26. RStudio Team. *RStudio: Integrated Development Environment for R*; Posit Software, PBC: Boston, MA, USA, 2024. Available online: https://posit.co/ (accessed on 4 January 2026).
27. O'Neill, M.E.; Mathews, K.L. Levene tests of homogeneity of variance for general block and treatment designs. *Biometrics* **2002**, *58*, 216–224. [CrossRef] [PubMed]
28. Urcelay, C.; Díaz, S.; Gurvich, D.E.; Chapin, F.S., III; Cuevas, E.; Domínguez, L.S. Mycorrhizal community resilience in response to experimental plant functional type removals in a woody ecosystem. *J. Ecol.* **2009**, *97*, 1291–1301. [CrossRef]

29. Bkhairia, I.; Mhamdi, S.; Jridi, M.; Nasri, M. New acidic proteases from *Liza aurata* viscera: Characterization and application in gelatin production. *Int. J. Biol. Macromol.* **2016**, *92*, 533–542. [CrossRef] [PubMed]
30. Hadidi, M.; Tarahi, M.; Günther Innerhofer, M.; Pitscheider, I.; Löscher, A.; Pignitter, M. Pumpkin seed as a sustainable source of plant-based protein for novel food applications. *Crit. Rev. Food Sci. Nutr.* **2025**, *65*, 8566–8591. [CrossRef]
31. Da Rocha, M.; Alemán, A.; Baccan, G.C.; López-Caballero, M.E.; Gómez-Guillén, C.; Montero, P.; Prentice, C. Anti-inflammatory, antioxidant, and antimicrobial effects of underutilized fish protein hydrolysate. *J. Aquat. Food Prod. Technol.* **2018**, *27*, 592–608. [CrossRef]
32. Hoa, N.T.Q.; Dao, D.T.A. Release bioactive peptides from enzymatic hydrolysated soybean by Alcalase and Protamex using response surface methodology. *Viet. J. Sci. Technol.* **2017**, *55*, 137–149. [CrossRef]
33. Innocente, N.; Calligaris, S.; Di Filippo, G.; Melchior, S.; Marino, M.; Nicoli, M.C. Process design for the production of peptides from whey protein isolate with targeted antimicrobial functionality. *Int. J. Food Sci. Technol.* **2023**, *58*, 2505–2517. [CrossRef]
34. Schlegel, K.; Sontheimer, K.; Hickisch, A.; Wani, A.A.; Eisner, P.; Schweiggert-Weisz, U. Enzymatic hydrolysis of lupin protein isolates—Changes in the molecular weight distribution, technofunctional characteristics, and sensory attributes. *Food Sci. Nutr.* **2019**, *7*, 2747–2759. [CrossRef]
35. Tacias-Pascacio, V.G.; Morellon-Sterling, R.; Siar, E.-H.; Tavano, O.; Berenguer-Murcia, Á.; Fernandez-Lafuente, R. Use of Alcalase in the production of bioactive peptides: A review. *Int. J. Biol. Macromol.* **2020**, *165*, 2143–2196. [CrossRef]
36. Peñuelas, J.; Gamon, J.A.; Fredeen, A.L.; Merino, J.; Field, C.B. Reflectance indices associated with physiological changes in nitrogen- and water-limited sunflower leaves. *Remote Sens. Environ.* **1995**, *48*, 135–146. [CrossRef]
37. Gamon, J.A.; Peñuelas, J.; Field, C.B. A narrow-waveband spectral index that tracks diurnal changes in photosynthetic efficiency. *Remote Sens. Environ.* **1992**, *41*, 35–44. [CrossRef]
38. Lardos, M.; Marmagne, A.; Bonadé Bottino, N.; Caris, Q.; Béal, B.; Chardon, F.; Masclaux-Daubresse, C. Discovery of the biostimulant effect of asparagine and glutamine on plant growth in *Arabidopsis thaliana*. *Front. Plant Sci.* **2024**, *14*, 1281495. [CrossRef] [PubMed]
39. Renzetti, M.; Funck, D.; Trovato, M. Proline and ROS: A unified mechanism in plant development and stress response? *Plants* **2025**, *14*, 2. [CrossRef] [PubMed]
40. Shehata, R.S. Proline in action: Enhancing fruit quality. *DYSONA–Appl. Sci.* **2025**, *6*, 8–15. [CrossRef]
41. Ávila, C.; Llebrés, M.T.; Cánovas, F.M.; Castro-Rodríguez, V. Arginine, a key amino acid for nitrogen nutrition and metabolism of forest trees. *J. Exp. Bot.* **2025**, *76*, 5238–5251. [CrossRef]
42. Sun, Y.; Miao, F.; Wang, Y.; Liu, H.; Wang, X.; Wang, H.; Guo, J.; Shao, R.; Yang, Q. L-Arginine alleviates the reduction in photosynthesis and antioxidant activity induced by drought stress in maize seedlings. *Antioxidants* **2023**, *12*, 482. [CrossRef]
43. Chen, Q.; Wang, Y.; Zhang, Z.; Liu, X.; Li, C.; Ma, F. Arginine Increases Tolerance to Nitrogen Deficiency in Malus hupehensis via Alterations in Photosynthetic Capacity and Amino Acids Metabolism. *Front. Plant Sci.* **2022**, *12*, 772086. [CrossRef]
44. Li, S.; Peng, F.; Xiao, Y.; Gong, Q.; Bao, Z.; Li, Y.; Wu, X. Mechanisms of high concentration valine-mediated inhibition of peach tree shoot growth. *Front. Plant Sci.* **2020**, *11*, 603067. [CrossRef]
45. Maillard, A.; Diquélou, S.; Billard, V.; Laîné, P.; Garnica, M.; Prudent, M.; Garcia-Mina, J.M.; Yvin, J.C.; Ourry, A. Leaf mineral nutrient remobilisation during leaf senescence and modulation by nutrient deficiency. *Front. Plant Sci.* **2015**, *6*, 317. [CrossRef]
46. Gao, Y.; Qin, Y.; Liu, Z.; Li, C.; Ma, F. Target of rapamycin (TOR) regulates the response to low nitrogen stress via autophagy and hormone pathways in *Malus hupehensis*. *Hortic. Res.* **2022**, *9*, uhac143. [CrossRef]
47. Fernández-Escobar, R.; Moreno, R.; García-Creus, M. Seasonal changes of mineral nutrients in olive leaves during the alternate-bearing cycle. *Sci. Hortic.* **1999**, *82*, 25–45. [CrossRef]
48. Shehzad, F.; Ali, Q.; Ali, S.; Al-Misned, F.A.; Maqbool, S. Fertigation with Zn-Lysine confers better photosynthetic efficiency and yield in water-stressed maize: Water relations, antioxidative defense mechanism and nutrient acquisition. *Plants* **2022**, *11*, 404. [CrossRef]
49. Okla, M.K.; Saleem, M.H.; Saleh, I.A.; Zomot, N.; Perveen, S.; Parveen, A.; Abasi, F.; Ali, H.; Ali, B.; Alwasel, Y.A.; et al. Foliar application of iron-lysine to boost growth attributes, photosynthetic pigments and biochemical defense system in canola (*Brassica napus* L.) under cadmium stress. *BMC Plant Biol.* **2023**, *23*, 648. [CrossRef] [PubMed]
50. Henderson, B.C.; Sanderson, J.M.; Fowles, A. A review of the foliar application of individual amino acids as biostimulants in plants. *Discov. Agric.* **2025**, *3*, 69. [CrossRef] [PubMed]
51. Alcazar, R.; Amorós Ortiz-Villajos, J.Á.; Pérez de los Reyes, C.; García Navarro, F.J.; Bravo Martín-Consuegra, S. Major and trace element content of olive leaves. *Olivæ* **2014**, *119*, 1–7. [CrossRef]
52. Osman, A.; Merwad, A.-R.M.; Mohamed, A.H.; Sitohy, M. Foliar spray with pepsin- and papain-whey protein hydrolysates promotes productivity of pea plants. *Molecules* **2021**, *26*, 2805. [CrossRef]
53. Ertani, A.; Schiavon, M.; Nardi, S. Transcriptome-wide identification of differentially expressed genes in *Solanum lycopersicon* L. in response to an alfalfa-protein hydrolysate using microarrays. *Front. Plant Sci.* **2017**, *8*, 1159. [CrossRef]

54. Hu, W.; Lu, Z.; Meng, F.; Li, X.; Cong, R.; Ren, T.; Sharkey, T.; Lu, J. The reduction in leaf area precedes that in photosynthesis under potassium deficiency: The importance of leaf anatomy. *New Phytol.* **2020**, *227*, 1749–1763. [CrossRef]
55. Wang, M.; Zheng, Q.; Shen, Q.; Guo, S. The critical role of potassium in plant stress response. *Int. J. Mol. Sci.* **2013**, *14*, 7370–7390. [CrossRef]
56. Sardans, J.; Peñuelas, J. Potassium control of plant functions: Ecological and agricultural implications. *Plants* **2021**, *10*, 419. [CrossRef]
57. Shabala, S.; Shabala, L. Ion transport and osmotic adjustment in plants and bacteria. *Biomol. Concepts* **2011**, *2*, 407–419. [CrossRef]
58. Liu, K.; Fu, H.; Bei, Q.; Luan, S. Inward potassium channel in guard cells as a target for polyamine regulation of stomatal movements. *Plant Physiol.* **2000**, *124*, 1315–1326. [CrossRef]
59. Agurla, S.; Gayatri, G.; Raghavendra, A.S. Polyamines increase nitric oxide and reactive oxygen species in guard cells of *Arabidopsis thaliana* during stomatal closure. *Protoplasma* **2018**, *255*, 153–162. [CrossRef]
60. Chabra, R.; Ringoet, A.; Lamberts, D. Kinetics and interaction of chloride and phosphate absorption by intact tomato plants (*Lycopersicon esculentum* Mill.) from a dilute nutrient solution. *Z. Pflanzenphysiol.* **1976**, *78*, 253–261. [CrossRef]
61. Hang, Z. Influence of chloride on the uptake and translocation of phosphorus in potato. *J. Plant Nutr.* **1993**, *16*, 1733–1737. [CrossRef]